Inertial shear bands in granular materials

Diego Berzi and James T. Jenkins

Inertial shear bands in granular materials

Diego Berzi[1,2] and James T. Jenkins[1]
[1]*Cornell University, Ithaca, New York 14853, USA*
[2]*Politecnico di Milano, Milano 20133, Italy*

We provide numerical solutions to the momentum and energy balance of a ki-
netic theory for the steady, collisional shearing of identical, inelastic, frictional
spheres between two different types of boundaries—rigid-bumpy and erodible, in
the absence of gravity. A rigid-bumpy boundary is a source of fluctuation energy
for the flow, an erodible boundary is a sink. As a consequence, the characteristics
of shearing between two rigid-bumpy boundaries, two erodible boundaries, and a
rigid-bumpy and an erodible boundary are all different. Here, we display these
differences and relate them to measurements of inhomogeneous shearing and the
development of shear bands in laboratory experiments. © 2015 AIP Publishing LLC.
[http://dx.doi.org/10.1063/1.4914920]

I. INTRODUCTION

We employ kinetic theory, extended to apply to very dense, very dissipative flows, to study
the steady collisional shearing of identical, inelastic, frictional spheres of diameter d between two
different types of boundaries—rigid-bumpy and erodible—in the absence of gravity. The theory
has already been successfully tested against experiments and discrete numerical simulations in a
number of flow configurations,[1–6] but here, we study its predictions on the developments of inertial
shear bands in which the transfer of momentum is dominated by collisions.

Typically, a shear band is a region of strong inhomogeneity bounded by regions of homogeneity
in a shearing flow. This is the situation in the boundary-value problem that we refer to as erod-
ible/erodible. Numerical simulations[7] and physical experiments[8] show the development of such a
band, although in the former case, it is not clear that collisions play a role in its development. We
also refer to the shearing flow between an erodible and a rigid, bumpy boundary as a shear band.
In the absence of gravity, the homogeneous region is in the center of a cell and the bands develop
adjacent to the rigid, bumpy boundaries. It is not uncommon to see this in numerical simulations.
When gravity is present, a single band develops near the upper boundary, as in the experiments of
Hanes and Inman.[9] Finally, we also consider shearing between two rigid, bumpy boundaries.

A rigid, bumpy boundary consists of a plane to which spheres, here identical to those of the
flow, have been fixed in a random array with some average spacing ℓ. The bumpiness, ψ, of the
boundary is defined as $\sin \psi = (d + \ell)/(2d)$. Collisions between flow spheres and boundary spheres
are dissipative, and the average slip velocity of the flow relative to the boundary and the conversion
of slip velocity to velocity fluctuations through collisions depends upon this dissipation and the
bumpiness of the boundary.

An erodible boundary is the interface between the collisional shearing flow and a denser
aggregate in which the shear rate is negligible. Collisions near the surface of this dense aggregate
dissipate energy and the erosion of spheres from its surface ensures that the velocity of the flow
relative to the interface vanishes. There is a flux of fluctuation energy into the flow at a rigid, bumpy
boundary and a flux of fluctuation out of the flow at an erodible boundary. As a consequence, the
characteristics of flows between two erodible and two rigid, bumpy boundaries are different; so also
are the characteristics of a shearing flow between a rigid-bumpy and an erodible boundary.

Here, we calculate profiles of mean velocity, volume fraction, and fluctuation energy flux and
predict the thickness of the shear band and the shear stress when the relative velocity between
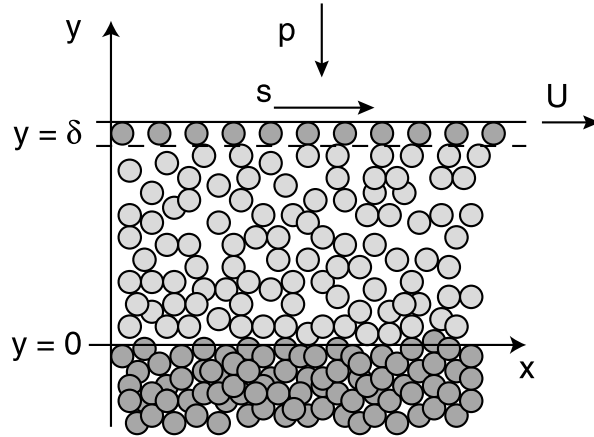
27, 033303-1

FIG. 1. Sketch of the flow configuration. Here, the particles are sheared between a rigid, bumpy, located at $y = \delta$, and an erodible boundary, located at $y = 0$.

the boundaries is varied at fixed pressure. We show that the inhomogeneity of shearing related to the nature of the boundaries is crucial in determining whether the ratio of shear stress to pressure increases or decreases with boundary velocity. We also indicate that the development of an erodible boundary in the interior of the flow in low velocity shearing between rigid, bumpy boundaries can explain the behaviour of the stress ratio versus inertial parameter seen in Ref. 10 and attributed by them to properties of the contacting surfaces.

II. THEORY

We take x and y to be the flow and shearing direction, respectively. The particles of density ρ, normal coefficient of restitution e, and contact friction μ, are sheared between two boundaries parallel to x, one at rest located at $y = 0$, and one moving at constant velocity U located at $y = \delta$ (Fig. 1). Then, u is the only component of the mean velocity of the particles, parallel to the boundaries. The local volume fraction of the particles is ν and we take it to be larger than 0.5 everywhere. We also introduce an effective coefficient of restitution ϵ to incorporate the role of contact friction in collisions, without the need of solving balances of angular momentum and rotational kinetic energy.[3,11]

In the absence of external forces, the particle pressure p, and shear stress, s, are constant. The balance of the fluctuation energy is

$$- Q' + su' - \Gamma = 0, \tag{1}$$

where Q is the flux of fluctuation energy and Γ its rate of collisional dissipation. Here, and in what follows, a prime indicates a derivative with respect to y. The first and second terms on the right-hand side of Eq. (1) are the diffusion of fluctuation energy associated with the random motion of the particles and the fluctuation energy produced by the work of the shear stress, respectively. Extended kinetic theory[12] in the dense limit provides constitutive relations for p, s, Γ, and Q

$$p = \rho f_1 T, \tag{2}$$

$$s = \rho d f_2 T^{1/2} u', \tag{3}$$

$$\Gamma = \rho \frac{f_3}{L} T^{3/2}, \tag{4}$$

and

$$Q = -\rho d f_4 T^{1/2} T'. \tag{5}$$

TABLE I. List of auxiliary coefficients in the constitutive relations of kinetic theory.

$f_1 = 2(1+e)\nu G$

$f_2 = \frac{8J}{5\pi^{1/2}}\nu G$

$f_3 = \frac{12}{\pi^{1/2}}\nu G(1-\epsilon^2)$

$f_4 = \frac{4M}{\pi^{1/2}}\nu G$

$G = \nu g_0$

$J = \frac{1+e}{2} + \frac{\pi}{4}\frac{(3e-1)(1+e)^2}{24-(1-e)(11-e)}$

$M = \frac{1+e}{2} + \frac{9\pi}{8}\frac{(2e-1)(1+e)^3}{(1+e)[16-7(1-e)]}$

$g_0 = \mathrm{f}\frac{2-\nu}{2(1-\nu)^3} + (1-\mathrm{f})\frac{2}{\nu_s-\nu}$

$\mathrm{f} = \frac{\nu^2 - 0.8\nu + \nu_s(0.8-\nu_s)}{0.8\nu_s - 0.16 - \nu_s^2}$

$f_0 = \left(\frac{f_2}{f_3}\right)^{1/2}\left[\frac{26(1-\epsilon)}{15}\left(\frac{\nu-0.49}{0.64-\nu}\right)+1\right]^{3/2}$

In these, T is the granular temperature (one-third of the mean square of the particle velocity fluctuations) and the coefficients f_i are explicit functions of the volume fraction and the micro-properties of the particles[13] and are given in Table I.

There, g_0 is the radial distribution function for contacting spheres, for which we adopt the expression introduced in Ref. 4 to reproduce the results of discrete numerical simulations.[14,15] In the dense limit, only terms proportional to g_0 in the coefficient functions are retained. The radial distribution function diverges at a value ν_s of the volume fraction, which can be interpreted as the limit beyond which a rate-independent component of the stresses develops. As shown in other discrete numerical simulations,[16] ν_s is a decreasing function of the contact friction of the particles.

In Eq. (4), the quantity L is a phenomenological correction to the dissipation rate,[17] to take into account the fact that, at volume fractions larger than roughly 0.49, the velocity distributions of two colliding particles are no longer uncorrelated.[14,18,19] The expression for L, which has the dimension of a length, is determined by a balance between the orienting influence of the shear rate and the randomizing influence of the collisions[20]

$$L = f_0\frac{u'd^2}{T^{1/2}}, \tag{6}$$

where f_0 is a dimensionless function of the volume fraction and the micro-properties of the particles (Table I). In discrete numerical simulations, the function f_0 is seen to diverge at $\nu = 0.64$, the volume fraction for a dense, random-packing of identical, frictional spheres; there is no observed dependence of the divergence of f_0 on e or μ.[4,5]

Upon differentiating Eq. (2) with respect to y, and using Eq. (5), we obtain

$$\nu' = \frac{Q}{\rho dT^{3/2}f_4(\ln f_1)_\nu}, \tag{7}$$

where the subscript indicates a derivative with respect to ν. Inverting Eq. (3), and using it in Eq. (1), permits us to obtain two further differential equations

$$u' = \frac{s}{\rho dT^{1/2}f_2} \tag{8}$$

and

$$Q' = \frac{s^2}{\rho dT^{1/2}f_2} - \Gamma. \tag{9}$$

The solution of the system of Eqs. (7) through (9), with $T = p/(\rho f_1)$ from Eq. (2), is obtained using the MATLAB solver "bvp4c" for two-point boundary-value problems. When appropriate boundary conditions are introduced, the solution provides profiles of volume fraction, velocity, and energy

flux through the depth of the flow. We consider situations in which the pressure is held fixed while the velocity U of the upper boundary is changed. The flow responds to changes in velocity by adjusting the gap δ. We treat the gap and the shear stress as additional unknowns of the problem, so that five boundary conditions are required.

At an erodible boundary, we employ the boundary conditions suggested in Ref. [21]—zero slip velocity, and an energy flux given by

$$Q_E = -2pT^{1/2}\left[\frac{3M(1-\epsilon)}{\pi L}\right]^{1/2},\tag{10}$$

modified to take into account the presence of L for dense flows. We assume that the transition to an erodible bed takes place when the compliance of the real spheres permits a rate-independent component of the stresses to develop. In discrete numerical simulations, this is seen to occur at a value of the volume fraction very close to ν_s.[22] Then, for shearing between two erodible boundaries (EE), the boundary conditions are $u(y=0) = u(y=\delta) = 0$, $Q(y=0) = -Q(y=\delta) = Q_E$, and $\nu(y=0) = 0.99\nu_s$. It must be emphasized that adopting the zero slip velocity as boundary condition neglects the possibility of creeping flow in the erodible bed.[23]

At a rigid, bumpy boundary, we employ the boundary conditions of Ref. [24]—a slip velocity given by

$$u_B = \left\{\frac{1-\left[5(1+e)/\left(2^{5/2}J\right)\right](1+B)\sin^2\psi}{(2/3)\left[2\csc^2\psi\left(\cos\psi\right)-\cos\psi\right]} + \frac{5(1+e)}{2^{3/2}J}\right\}\left(\frac{\pi}{2}\right)^{1/2}\frac{s}{p}T^{1/2},\tag{11}$$

where $B = \pi\left[1 + 5/(8G)\right]/\left(2^{1/2}12\right)$; and an energy flux given as

$$Q_B = su_B - \frac{2^{3/2}(1-\cos\psi)\csc^2\psi}{\pi^{1/2}}\frac{1-\epsilon}{L}pT^{1/2}.\tag{12}$$

Consequently, for shearing between two rigid-bumpy boundaries (BB), the boundary conditions are $u(y=0) = u_B$, $u(y=\delta) = U - u_B$, $Q(y=0) = -Q(y=\delta) = Q_B$, and we specify the number hold-up H—the number of flowing particles in the shear band over a unit area of the boundary: $H = 6/\pi \int_0^\delta \nu \, dy$.

Finally, for shearing between a rigid-bumpy and an erodible boundary (BE), the boundary conditions are $u(y=0) = 0$, $u(y=\delta) = U - u_B$, $Q(y=0) = Q_E$, $Q(y=\delta) = -Q_B$, and $\nu(y=0) = 0.99\nu_s$.

III. NUMERICAL SOLUTIONS

Unless explicitly stated, the results shown have been obtained with coefficient of restitution $e = 0.7$ and coefficient of sliding friction $\mu = 0.5$, so that the effective coefficient of restitution is 0.53 and $\nu_s = 0.587$.[3,16] In the flows between two bumpy-rigid boundaries and between a bumpy-rigid and an erodible boundary, we employ a bumpiness, ψ equal to $\pi/4$; in the BB flows, the number of particles per unit area, H, is equal to ten. We phrase our results in terms of the ratio between the shear stress and the pressure and the boundary velocity made dimensionless by the square root of the ratio of the pressure to the particle density. We consider the range of $U/(p/\rho)^{1/2}$ between 0.1 and 3, in which the flow is inertial, but very dense. We obtain, in all cases, a substantially linear velocity profile in the shearing layer, with non-zero slip velocity at rigid, bumpy boundaries and rather uniform profiles of granular temperature and volume fraction, with ν close to ν_s. The ratio of $U/(p/\rho)^{1/2}$ to the thickness of the shear band δ is the inertial parameter.[25] Most of our results are in a range of inertial parameter between 0.002 and 0.2.

We first analyse the results for shearing between two erodible boundaries. Figure 2 shows that the stress ratio decreases with increasing velocity and asymptotically approaches the yield stress ratio for large $U/(p/\rho)^{1/2}$. This is the value of the stress ratio in steady, homogeneous (simple) shearing at which a rate-independent component of the stresses develops. The thickness δ of the shear band in terms of particle diameters increases linearly with $U/(p/\rho)^{1/2}$, with a slope of about 30.
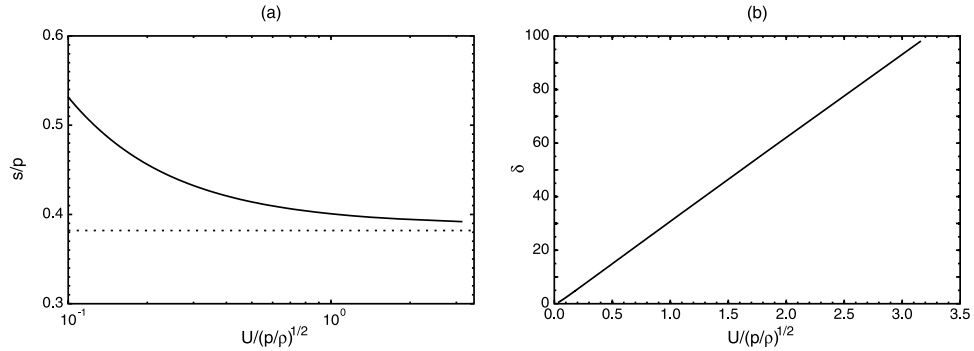
FIG. 2. (a) Stress ratio and (b) thickness of the shear band as functions of the dimensionless boundary velocity in flows between erodible boundaries at fixed pressure. Also shown (dotted line) is the value of the yield stress ratio for simple shearing.[16]

Erodible boundaries are dissipative, so that the energy flux is directed out of the flow into the boundaries. Consequently, the shear stress has to increase with respect to that in simple shearing, so that the internal production of fluctuation energy compensates for the additional energy loss. However, as the thickness of the shear band increases, the influence of the boundaries progressively diminishes, and the stress ratio tends to the value at simple shearing. This velocity weakening of an inertial shear band is due entirely to the nature of the boundaries and may explain the reduction of friction with slip velocity in granular fault zones.[26,27]

We next consider a granular material sheared between a rigid, bumpy boundary and an erodible boundary. Figure 3 shows the stress ratio s/p and the thickness of the shear band δ as functions of $U/(p/\rho)^{1/2}$. Also shown are the results for a lower bumpiness $\psi = \pi/6$ and a lower contact friction $\mu = 0.1$, for which we take $\epsilon = 0.59$ and $\nu_s = 0.613$.[3,16] As in the erodible-erodible flows, the dimensionless thickness increases linearly with $U/(p/\rho)^{1/2}$, with a slope between 30 and 45. The relation between the stress ratio and the relative boundary velocity depends strongly on both the bumpiness and the contact friction.

For relatively large bumpiness and contact friction ($\psi = \pi/4$ and $\mu = 0.5$), there is velocity weakening; if the bumpiness is decreased ($\psi = \pi/6$), there is a change to velocity strengthening, which can be changed again into a mild velocity weakening by lowering the contact friction ($\mu = 0.1$). In any case, the stress ratio asymptotically approaches the value associated with simple shearing for large $U/(p/\rho)^{1/2}$.

Once again, the behaviour of the stress ratio can be understood from a consideration of the energetics. Erodible boundaries are dissipative, so they take energy from the interior of the flow;
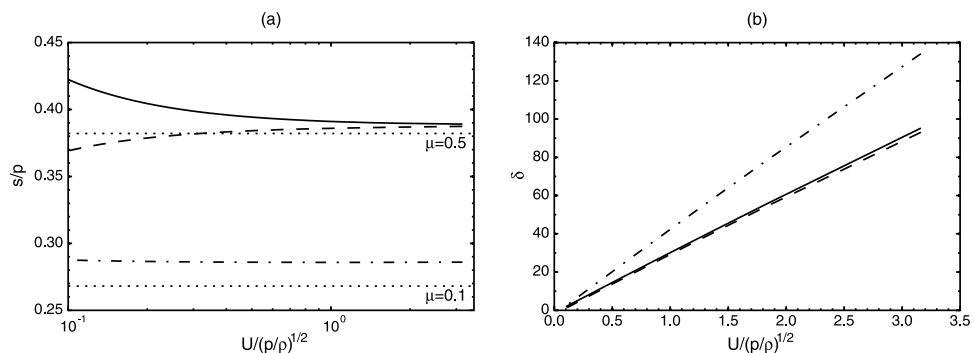

FIG. 3. (a) Stress ratio and (b) thickness of the shear band as functions of the dimensionless boundary velocity in flows between a rigid-bumpy and an erodible boundary at fixed pressure for $\psi = \pi/4$ and $\mu = 0.5$ (solid line); $\psi = \pi/6$ and $\mu = 0.5$ (dashed line); $\psi = \pi/6$ and $\mu = 0.1$ (dotted-dashed lines). Also shown (dotted lines) are the values of the yield stress ratio for simple shearing.[16]
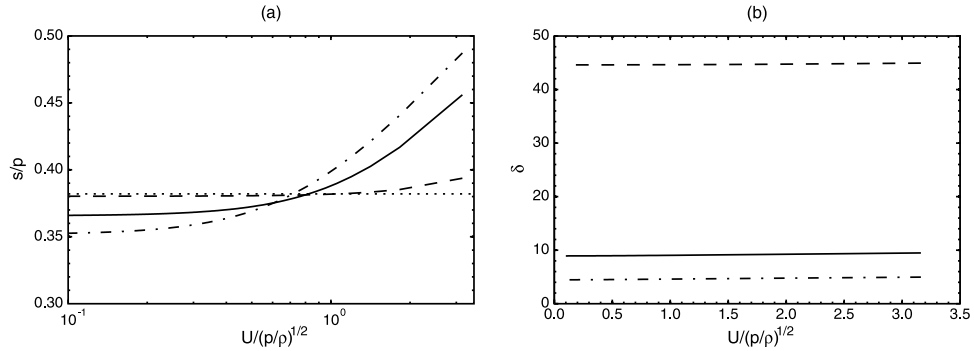
FIG. 4. (a) Stress ratio and (b) thickness of the shear band as functions of the dimensionless boundary velocity for flows between rigid-bumpy boundaries at fixed pressure for: $H = 10$ (solid line), $H = 50$ (dashed line), and $H = 5$ (dotted-dashed line). Also shown (dotted line) is the value of the yield stress ratio for simple shearing.[16]

rigid, bumpy boundaries are energetic, so that they add energy to the interior of the flow. The excess or deficiency of the rate of working of the stresses over the rate of dissipation in the interior required by the boundary fluxes determines whether there must be an increase or decrease in the shear stress over that in simple shear. Again, as the thickness of the shear band increases, the influence of the boundaries on the flow progressively diminishes, and the stress ratio tends to the value at simple shearing. In this case, this value is always larger than the yield value because the asymptotic volume fraction is less than ν_s.

We finally consider a granular material sheared between two rigid-bumpy boundaries. Figure 4 shows the stress ratio s/p and the thickness of the shear band δ as functions of $U/(p/\rho)^{1/2}$ when the granular material is sheared at fixed pressure for three different values of the number hold-up H. The stress ratio always increases with $U/(p/\rho)^{1/2}$ and asymptotically approaches a constant value less than that at simple shearing for small $U/(p/\rho)^{1/2}$. Unlike the other flows, the thickness δ is only a weakly increasing function of the relative boundary velocity and increases with H, from roughly five diameters at $H = 5$ to 45 diameters at $H = 50$. This weak dependence on the relative boundary velocity is characteristic of the small values of $U/(p/\rho)^{1/2}$—large values of volume fraction—that we focus on. For larger values of $U/(p/\rho)^{1/2}$—smaller values of volume fraction— the thickness of the shear band is a more strongly increasing function of the relative boundary velocity. Also, Fig. 5 shows that at larger values of $U/(p/\rho)^{1/2}$, the profiles of granular temperature and volume fraction have a much stronger curvature, while the velocity profile is S-shaped.[4]

Rigid, bumpy boundaries are energetic and provide fluctuation energy to the interior. Consequently, the corresponding correction to the stress ratio of simple shearing is always negative. That is, the shear stress is less than that at simple shearing because less internal production of fluctuation
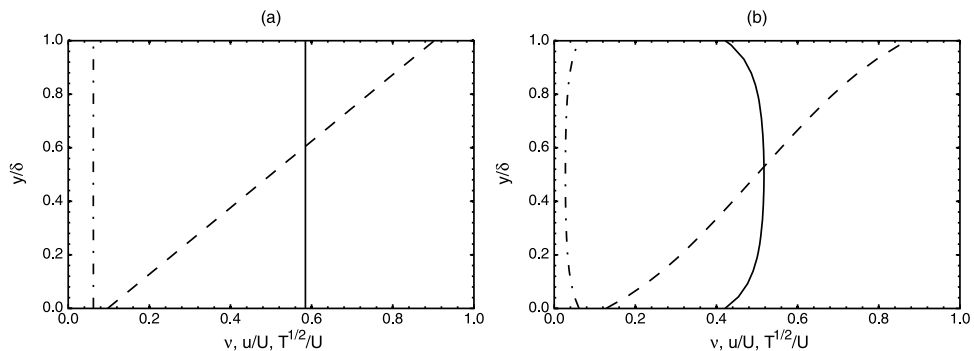

FIG. 5. Profiles of volume fraction (solid lines), normalized velocity (dashed lines), and normalized square root of granular temperature (dotted-dashed lines) in flows between two rigid-bumpy boundaries for $H = 10$ and (a) $U/(p/\rho)^{1/2} = 0.5$; (b) $U/(p/\rho)^{1/2} = 9.5$.
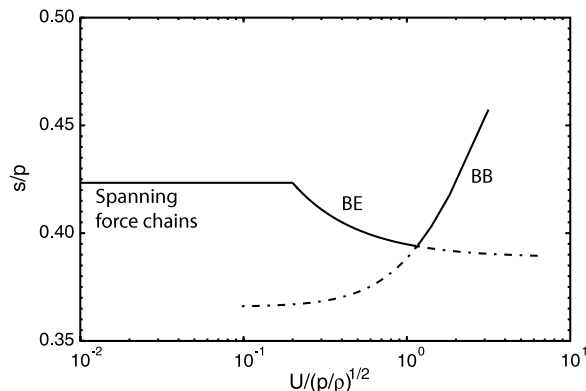
FIG. 6. Stress ratio as a function of the dimensionless boundary velocity in a possible transition from a flow between two bumpy-rigid boundaries and that between a rigid-bumpy and an erodible boundary.

energy is required. Also, as the distance between the boundaries remains constant, the influence of the boundaries on the flow progressively diminishes as the relative velocity between the boundaries decreases.

The loading of a flow of constant thickness plays a role similar to the increase of thickness of a flow of constant loading—it diminishes the role of the boundary flux relative the production or dissipation of energy in the interior. In the flows considered here, the energy flux from the boundaries is more than ten per cent of the rate of production in the interior for hold-up H less than 20. Hence, the low-velocity asymptote of the stress ratio is less than the yield value in simple shearing, and decreases further as the thickness of the flow decreases. This flux of fluctuation energy may partially explain why flows at values of the stress ratio less than the yield value in simple shearing have been observed in discrete numerical simulations.[28] They have been modelled by Kamrin and co-workers by introducing a second-order boundary-value problem for the rate of shear.[29,30] The collisional model that we employ does not take into account a rate-independent component of the stresses. However, the two approaches should agree when only collisional interactions are present. In this case, the equations of Kamrin *et al.*[29,30] can be obtained from ours by using the constitutive relation for the stress to eliminate the temperature from the energy balance in favor of the shear rate.

When we reduce the relative boundary velocity at a constant number hold-up in the BB case, the average volume fraction increases. In absence of gravity, the profile of volume fraction has a maximum at $y = \delta/2$. When the local value of the volume fraction at $y = \delta/2$ is exactly equal to ν_s, the region between the two rigid-bumpy boundaries splits into an inner erodible bed and two outer shear bands, each enclosed between a rigid-bumpy and an erodible boundary. In this case, the thickness of the erodible bed Δ is related to the thickness of the shear band in the BE case, δ, through H: $H = 12/\pi \int_0^\delta \nu \mathrm{d}y + 6\nu_s \Delta/\pi$, if we assume that the volume fraction in the erodible bed is constant and equal to ν_s. When the thickness of each of the outer shear bands is less than one diameter, that is, for U less than a certain value, the force chains that extend into the erodible bed are in contact with the rigid, bumpy boundaries, giving rise to a rate-independent regime.

The behaviour of the stress ratio with $U/(p/\rho)^{1/2}$ at $H = 10$ in an idealized experiment is shown in Fig. 6. At small relative boundary velocity, the force chains span the entire domain and the stress ratio is independent of the velocity. When the velocity increases beyond a certain value, two shear bands between the rigid-bumpy and erodible boundaries develop. By increasing U further, Δ decreases; when Δ vanishes, the two symmetric bumpy-erodible flows become a bumpy-bumpy flow. The combination of the velocity weakening of the bumpy-erodible case and the velocity strengthening of the bumpy-bumpy case results in a non-monotonic relation between the stress ratio and the relative boundary velocity, and the presence of a minimum, as in the experiments.[10]

The experiment differs from the idealized situation that we have described in several ways. First of all, gravity acts along the direction perpendicular to the boundaries. This causes a breaking in the symmetry of the problem, so that in the transition from the BB to the BE case, the erodible

bed would develop at the bottom, and only one shear band between a rigid-bumpy and an erodible boundary would be present at the top. Second, in the experiments, the flow takes place between vertical sidewalls that provide an additional resistance force, and further symmetry-breaking of the problem. Third, the erodible bed creeps, and the velocity profile there is exponential.[23] The few experimental points in the velocity profiles reported by Kuwano, Ando, and Hatano[10] are not sufficient to assess or rule out the transition from a BB to a BE flow in that case.

IV. CONCLUSIONS

We have obtained numerical solutions for steady, uniform, inhomogeneous shearing flows between three combinations of rigid-bumpy and erodible boundaries at fixed pressure. From these, we calculated the relationship between the ratio of the components of stress tangent and normal to the boundary versus the relative boundary velocity normalized by a measure of the pressure. Inhomogeneity in the flow profiles related to the type of boundary influence this relationship.

Flows between pairs of erodible boundaries always show velocity weakening; while those between pairs of rigid, bumpy boundaries always show velocity strengthening. Bumpy-erodible flows show velocity weakening for bumpiness larger than a certain value, which increases with contact friction, and velocity strengthening for smaller bumpiness.

The stress ratio approaches an asymptotic value at large velocities in the erodible-erodible and bumpy-erodible flows and at small velocities in the bumpy-bumpy flows. The asymptotic value of the stress ratio is larger than the yield stress ratio in simple shearing for the erodible-erodible and bumpy-erodible flows, but is less than the yield stress ratio in the bumpy-bumpy flows, in which it increases if the number of particles per unit area of the boundary increases.

In a transition between bumpy-bumpy and bumpy-erodible flows, the relationship between the stress ratio and the relative boundary velocity is not monotone and exhibits a minimum similar to that seen in Ref. 10 and attributed by them to properties of the contacting surfaces.

[1] J. Jenkins and D. Berzi, "Kinetic theory applied to inclined flows," Granular Matter **14**, 79–84 (2012).

[2] D. Berzi and J. T. Jenkins, "Surface flows of inelastic spheres," Phys. Fluids **23**, 013303 (2011).

[3] M. Larcher and J. Jenkins, "Segregation and mixture profiles in dense, inclined flows of two types of spheres," Phys. Fluids **25**, 113301 (2013).

[4] D. Vescovi, D. Berzi, P. Richard, and N. Brodu, "Plane shear flows of frictionless spheres: Kinetic theory and 3D soft-sphere discrete element method simulations," Phys. Fluids **26**, 053305 (2014).

[5] D. Berzi and D. Vescovi, "Different singularities in the functions of extended kinetic theory at the origin of the yield stress in granular flows," Phys. Fluids **27**, 013302 (2015).

[6] H. Xu, M. Louge, and A. Reeves, "Solutions of the kinetic theory for bounded collisional granular flows," Continuum Mech. Thermodyn. **15**, 321–349 (2003).

[7] C. Thornton and L. Zhang, "A numerical examination of shear banding and simple shear non-coaxial flow rules," Philos. Mag. **86**, 3425–3452 (2006).

[8] B. Szabó, J. Török, E. Somfai, S. Wegner, R. Stannarius, A. Böse, G. Rose, F. Angenstein, and T. Börzsönyi, "Evolution of shear zones in granular materials," Phys. Rev. E **90**, 032205 (2014).

[9] D. Hanes and L. Inman, "Observations of rapidly flowing granular-fluid materials," J. Fluid Mech. **150**, 357–380 (1985).

[10] O. Kuwano, R. Ando, and T. Hatano, "Crossover from negative to positive shear rate dependence in granular friction," Geophys. Res. Lett. **40**, 1295–1299, doi: 10.1002/grl.50311 (2013).

[11] J. Jenkins and C. Zhang, "Kinetic theory for identical, frictional, nearly elastic spheres," Phys. Fluids **14**, 1228–1235 (2002).

[12] J. T. Jenkins and D. Berzi, "Dense inclined flows of inelastic spheres: Tests of an extension of kinetic theory," Granular Matter **12**, 151–158 (2010).

[13] V. Garzó and J. W. Dufty, "Dense fluid transport for inelastic hard spheres," Phys. Rev. E **59**, 5895 (1999).

[14] N. Mitarai and H. Nakanishi, "Velocity correlations in the dense granular shear flows: Effects on energy dissipation and normal stress," Phys. Rev. E **75**, 031305–031313 (2007).

[15] S. Chialvo and S. Sundaresan, "A modified kinetic theory for frictional granular flows in dense and dilute regimes," Phys. Fluids **25**, 070603 (2013).

[16] S. Chialvo, J. Sun, and S. Sundaresan, "Bridging the rheology of granular flows in three regimes," Phys. Rev. E **85**, 021305 (2012).

[17] J. T. Jenkins, "Dense shearing flows of inelastic disks," Phys. Fluids **18**, 103307 (2006).

[18] N. Mitarai and H. Nakanishi, "Bagnold scaling, density plateau, and kinetic theory analysis of dense granular flow," Phys. Rev. Lett. **94**, 128001 (2005).

[19] V. Kumaran, "Dynamics of dense sheared granular flows. Part II. The relative velocity distributions," J. Fluid Mech. **632**, 145–198 (2009).

[20] J. T. Jenkins, "Dense inclined flows of inelastic spheres," Granular Matter **10**, 47–52 (2007).

[21] J. Jenkins and E. Askari, "Boundary conditions for rapid granular flows: Phase interfaces," J. Fluid Mech. **223**, 497–508 (1991).

[22] S. Ji and H. H. Shen, "Internal parameters and regime map for soft polydispersed granular materials," J. Rheol. **52**, 87–103 (2008).

[23] T. Komatsu, S. Inagaki, N. Nakagawa, and S. Nasuno, "Creep motion in a granular pile exhibiting steady surface flow," Phys. Rev. Lett. **86**, 1757–1760 (2001).

[24] M. Richman, "Boundary conditions based on a modified maxwellian velocity distribution function for flows of identical, smooth, nearly elastic spheres," Acta Mech. **75**, 227–240 (1988).

[25] GDR-MiDi, "On dense granular flows," Eur. Phys. J. E **14**, 341–365 (2004).

[26] G. Zheng and J. Rice, "Conditions under which velocity-weakening friction allows a self-healing versus a cracklike mode of rupture," B. Seismol. Soc. Am. **88**, 1466–1483 (1998).

[27] D. Faulkner, C. Jackson, R. Lunn, R. Schlische, Z. Shipton, and C. Wibberley, "A review of recent developments concerning the structure, mechanics and fluid flow properties of fault zones," J. Struct. Geol. **32**, 1557–1575 (2010).

[28] G. Koval, J.-N. Roux, A. Corfdir, and F. Chevoir, "Annular shear of cohesionless granular materials: From the inertial to quasistatic regime," Phys. Rev. E **79**, 021306 (2009).

[29] K. Kamrin and G. Koval, "Nonlocal constitutive relation for steady granular flow," Phys. Rev. Lett. **108**, 178301 (2012).

[30] D. Henann and K. Kamrin, "A predictive, size-dependent continuum model for dense granular flows," Proc. Natl. Acad. Sci. U. S. A. **110**, 6730–6735 (2013).